DOI: 10.1002/cssc.201200914

Conversion of Cellulose and Cellobiose into Sorbitol Catalyzed by Ruthenium Supported on a Polyoxometalate/Metal–Organic Framework Hybrid

Jinzhu Chen,*[a] Shengpei Wang,[a, c] Jing Huang,[a] Limin Chen,*[b] Longlong Ma,[a] and Xing Huang[a]

Cellulose and cellobiose were selectively converted into sorbitol over water-tolerant phosphotungstic acid (PTA)/metal–organic-framework-hybrid-supported ruthenium catalysts, Ru-PTA/MIL-100(Cr), under aqueous hydrogenation conditions. The goal was to investigate the relationship between the acid/metal balance of bifunctional catalysts Ru-PTA/MIL-100(Cr) and their performance in the catalytic conversion of cellulose and cellobiose into sugar alcohols. The control of the amount and strength of acid sites in the supported PTA/MIL-100(Cr) was achieved through the effective control of encapsulated-PTA loading in MIL-100(Cr). This design and preparation method led to an appropriately balanced Ru-PTA/MIL-100(Cr) in terms of Ru dispersion and hydrogenation capacity on the one hand, and acid site density of PTA/MIL-100(Cr) (responsible for acid-catalyzed hydrolysis) on the other hand. The ratio of acid site density to the number of Ru surface atoms (n_A/n_{Ru}) of Ru-PTA/MIL-100(Cr) was used to monitor the balance between hydrogenation and hydrolysis functions; the optimum balance between the two catalytic functions, that is, $8.84 < n_A/n_{Ru} < 12.90$, achieves maximum conversion of cellulose and cellobiose into hexitols. Under the applied reaction conditions, optimal results (63.2% yield in hexitols with a selectivity for sorbitol of 57.9% at complete conversion of cellulose, and 97.1% yield in hexitols with a selectivity for sorbitol of 95.1% at complete conversion of cellobiose) were obtained using a Ru-PTA/MIL-100(Cr) catalyst with loadings of 3.2 wt% for Ru and 16.7 wt% for PTA. This research thus opens new perspectives for the rational design of acid/metal bifunctional catalysts for biomass conversion.

Introduction

The application of heterogeneous catalysis and the use of renewable feedstock in chemical synthesis are core themes of green and sustainable chemistry;[1] therefore, the catalytic routes to fine chemicals and fuels from renewable resources have attracted considerable attention over the last few years.[2] Cellulose presents the most abundant renewable and non-edible biopolymer, the major fraction of which (around 40%) is lignocellulose.[3–8] Cellulose can be converted into sugar alcohols,[9–28] ethylene glycol (EG),[29–31] oxygenated bio-oil,[32] and hydrocarbons[33] through various chemical transformations.[3–8] Especially sorbitol, which is the hydrogenated form of glucose, is targeted herein because it is a good model system to study both hydrolysis and hydrogenation (Scheme 1). Sorbitol is widely used as a sweetener, a moisture controller in cosmetics, and in medical applications. It also has been studied as a resource for the production of hydrogen,[33] alkanes,[34,35] and value-added chemicals.[36,37]

A historical retrospect of the progress of hydrolytic hydrogenation of cellulose into sorbitol reveals that most of the catalytic systems used share two main components (Scheme 1): 1) a transition-metal catalyst (often Pt or Ru) and 2) a dilute acid or a solid support with sufficient acidity (e.g., oxidized carbon, silica–alumina, or acidic zeolites).[21–28] A good balance between the two catalytic functions is a necessity.[26] Furthermore, the development of more efficient solid-acid materials is the key to improve the performance of a bifunctional heterogeneous catalyst for sorbitol formation.[24]

Polyoxometalates (POMs), such as Keggin-type phosphotungstic acid (PTA, $H_3PW_{12}O_{40}$), may possess acidity even stronger than H_2SO_4.[27,28,38] A few studies have shown that PTA is active for the hydrolysis or alcoholysis of cellobiose or cellulose.[39,40] However, in these systems, POMs functioned homogeneously in the liquid phase, and the separation and recovery of the catalyst from the product and the reaction medium would be problematic. Therefore, water-tolerant $Cs_xH_{3-x}PW_{12}O_{40}$-supported Ru nanoparticles were developed as bifunctional catalysts for the conversion of cellobiose and cellulose into sorbitol in aqueous media.[24] Another main limita-

[a] Prof. Dr. J. Chen, S. Wang, J. Huang, Prof. Dr. L. Ma, Dr. X. Huang
Key Laboratory of Renewable Energy and Natural Gas Hydrate
Guangzhou Institute of Energy Conversion
Chinese Academy of Sciences
Guangzhou 510640 (PR China)
Fax: (+86) 20-3722-3380
E-mail: chenjz@ms.giec.ac.cn

[b] Dr. L. Chen
College of Environment and Energy
South China University of Technology
Guangzhou 510006 (PR China)
E-mail: liminchen@scut.edu.cn

[c] S. Wang
Graduate University of Chinese Academy of Sciences
Beijing 100049 (PR China)

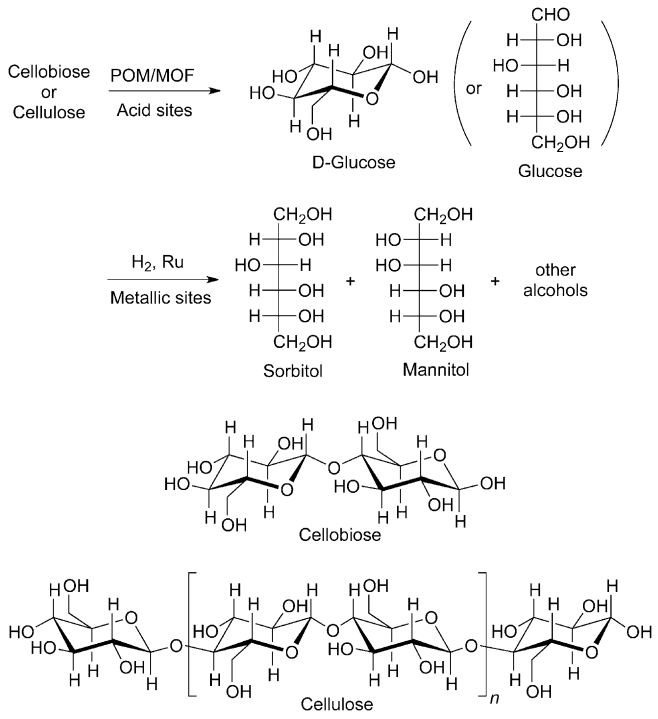

Scheme 1. Conversion of cellobiose and cellulose into sorbitol.

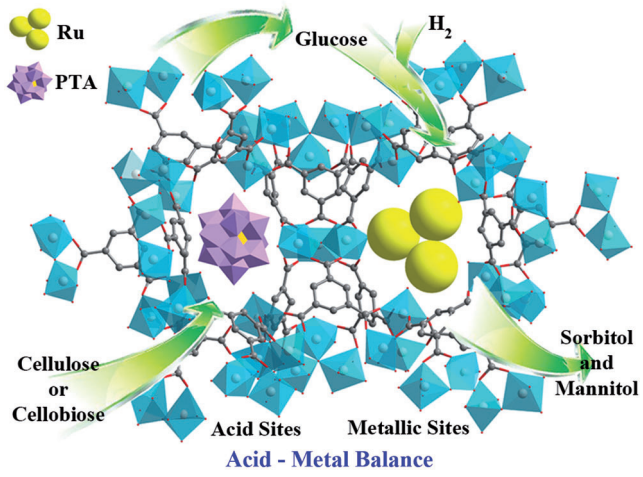

Figure 1. Metal–acid bifunctional catalyst Ru-PTA/MIL-100(Cr).

tion of POMs ($Cs_xH_{3-x}PW_{12}O_{40}$) as acidic catalysts is their small surface area (1–10 $m^2 g^{-1}$) and low porosity (<0.1 $cm^3 g^{-1}$).[41–42] Therefore, the applications of POMs as solid acid catalysts are limited. Various high-surface-area supports, such as silica, activated carbon, ion-exchange resin, and mesoporous molecular sieves, have been used for POM dispersion. However, these systems are often regarded as ill-defined with many limitations, including low POM loading, POM leaching, the conglomeration of POM particles, active sites that are nonuniform, and the deactivation of acid sites by water. The immobilization of POMs in a suitable solid matrix, which can overcome these drawbacks, is a step toward the challenging goal of catalysis.

Following the so-called "ship in a bottle" approach, the encapsulation of POMs in the mesoporous cavities of metal–organic frameworks (MOFs) can be used to synthesize a highly dispersed POM/MOF hybrid material with both outstanding Brønsted acidity and high surface area (up to 1080 $m^2 g^{-1}$).[41–45] These POM/MOF hybrids showed higher stability and reusability than other supported Keggin-type POMs. Moreover, most POM/MOF hybrids were water-tolerant and exhibiedt higher activity than the zeolite H-ZSM-5 (ZSM = zeolite Socony Mobil) for acid-catalyzed reactions in water.[43] Another important advantage of POM/MOF hybrids is that the control of the amount and strength of acid sites in POM/MOF materials can be readily achieved by the effective control of encapsulated-POM loadings in MOFs. Thus, as metal–acid bifunctional catalysts, POM/MOF-hybrid-supported metal catalysts (M-POM/MOF with M = Ru, Pt, Rh, Pd) provide an ideal model to investigate the balance between the activity of acid sites in the hydrolysis and the activity of metallic sites in the hydrogenation of cellobiose and cellulose and their conversion into sorbitol (Figure 1). Moreover, the high-surface-area MOFs show equivalent or even better adsorption capacity of hydrogen than zeolites or activated carbon; the use of MOF-supported metal catalysts should thus facilitate hydrogen activation in hydrogenation reactions.[46]

However, few studies on cellulose or cellobiose conversion using heterogeneous POM/MOF hybrid catalysts have been undertaken to date. Herein, we report a first study on the exploitation of PTA/MIL-100(Cr)-hybrid-supported Ru nanoparticles for the conversion of cellobiose and cellulose into sorbitol in water (Figure 1). Furthermore, the appropriate balance between the hydrogenation and hydrolysis functions of the metal–acid bifunctional catalyst Ru-PTA/MIL-100(Cr) is systematically evaluated.

Results and Discussion

Bifunctional heterogeneous catalysts

Cellulose and cellobiose undergo hydrolysis followed by hydrogenation according to the sequence: cellulose (cellobiose)→glucose→sorbitol (Scheme 1). Therefore, a bifunctional catalyst combining hydrolysis and hydrogenation functions is required for the formation of sorbitol from cellulose and cellobiose (Figure 1).

The direct encapsulation of PTA in MIL-100(Cr) was performed by the addition of PTA to the MIL-100(Cr) synthesis mixture to yield PTA/MIL-100(Cr).[44] Thermogravimetric analysis revealed that both MIL-100(Cr) and PTA/MIL-100(Cr) are stable up to 327 °C in air;[44] thus, the chosen temperature of up to 200 °C for the hydrolytic hydrogenation of cellobiose and cellulose is suitable to ensure the stability of Ru-PTA/MIL-100(Cr). Ru-PTA/MIL-100(Cr) was prepared through a conventional impregnation of an aqueous solution of $RuCl_3$ into PTA/MIL-100(Cr), followed by hydrogen reduction at 160 °C. The supported Ru catalyst was recovered by filtration, washed with deionized water, and dried at 100 °C.

Sorbitol is the major product of the hydrolytic hydrogenation of cellobiose and cellulose. Sorbitol and mannitol

(Scheme 1) are known to be produced through the hydrogenation of glucose and mannose, respectively; in the literature, the formation of mannose is attributed to the acid-catalyzed C2 epimerization of glucose.[47] Furthermore, EG, glycerol, 1,2-propanediol, and other low molecular weight polyols were shown to originate from metal-catalyzed hydrogenolysis.[29–31] Although not always mentioned, a multitude of by-products can be formed during the metal-catalyzed cracking of cellulose.[48] For the sake of clarity, only the amounts of sorbitol, mannitol, glycerol, and EG are plotted here.

Cellobiose conversion into sorbitol

Because of the robust crystalline structure of cellulose, its catalytic transformation is a challenging task. Cellobiose is a dimer of glucose molecules connected through a glycosidic bond and represents the simplest model molecule for cellulose (Scheme 1);[10,14,24] the conversion of cellobiose was thus carried out to provide useful insights into the rational design of efficient catalysts for cellulose transformations.

We started out with the hydrolytic hydrogenation of cellobiose under pressurized hydrogen conditions in water using Ru-PTA/MIL-100(Cr) as a bifunctional catalyst. The effect of reaction temperature on sorbitol yields was investigated first. A complete cellobiose hydrolysis and sequential glucose hydrogenation was observed between 140 and 160 °C (Table 1, runs 1–4). Sorbitol yields increased as the temperature increased to a maximum of 95.1% at 150 °C. A further increase in temperature to 160 °C, however, led to a slightly reduced sorbitol yield of 80.8%, indicating acid-catalyzed sorbitol degradation at higher reaction temperatures.

Different amounts of Ru were loaded on PTA/MIL-100(Cr) (PTA = 16.7 wt%) support, and the effect of the amount of Ru on sorbitol yields was also studied (Table 1, runs 5–10). The use of Ru-PTA/MIL-100(Cr) with a Ru loading of 1.2 wt% produced sorbitol with a yield of only 23.4%, whereas glucose (3.2%) was also detected. In this case, the amount of Ru seemed to be insufficient to fully hydrogenate glucose into sorbitol. Furthermore, a combined analysis of data from experiments with different loading amounts suggested that Ru-PTA/MIL-100(Cr) with a Ru and PTA loading of 3.2 and 16.7 wt%, respectively, showed the highest sorbitol yield and the highest selectivity for sorbitol. These results indicate that a balanced Ru/PTA ratio is important for the effective conversion of cellobiose into sorbitol.

In the cases in which MIL-100(Cr) (Table 1, run 11) and PTA/MIL-100(Cr) (Table 1, run 12) were used as catalysts directly, no sugar alcohols were observed, although cellobiose conversions were approximately 33.2% for MIL-100(Cr) and 41.4% for PTA/MIL-100(Cr). Under the above conditions, glucose was predominantly produced by hydrolysis of cellobiose with MIL-100(Cr) as a Lewis acid and PTA/MIL-100(Cr) as a Brønsted acid. However, when Ru/MIL-100(Cr) (Table 1, run 13) was used as a catalyst, a complete cellobiose conversion with a mediocre yield in sorbitol of 56.0% was observed, which is in sharp contrast with catalyst Ru-PTA/MIL-100(Cr), which achieved a yield in sorbitol of 95.1% (Table 1 run 2). These results further demonstrate that a good balance between the two catalytic functions (i.e., the strength of acid sites and the activity of the hydrogenation metallic sites) is important.

Cellulose conversion into sorbitol

Ru-PTA/MIL-100(Cr) was further exploited for the conversion of cellulose in aqueous media. The transformation of cellulose into sorbitol consists of the hydrolysis of cellulose to glucose via water-soluble oligosaccharides and the successive hydrogenation of glucose to sorbitol (Scheme 1).[14]

Cellulose has crystalline and amorphous parts in its structure. The conversion of the crystalline region into an amorphous one provides higher reactivity to cellulose. Various methods have been reported for the pretreatment of cellulose to reduce crystallinity and enhance contact between the catalysts and cellulose;[13,15] in our case, ball millling was selected for this purpose. Commercial cellulose exhibited strong diffraction peaks at 2θ of 15.0°, 16.0°, and 22.5°, which are characteristic diffractions of the (101), (10$\bar{1}$), and (002) planes in the cellulose I crystal. Figure 2 depicts the change in XRD diffraction peaks of cellulose after pretreatment. The intensity of the (002) diffraction at 22.5° clearly decreased with treatment. The crystallinity index (CrI) of cellulose was 75% for nontreated, 16% for cellulose pretreated for 2000 min, and 10% for cellulose pretreated for 3000 min, estimated from the intensity difference of the (002) diffraction and that of the amorphous part.[15,49] The

Table 1. Effect of reaction temperature and catalyst composition on cellobiose conversion into sorbitol.[a]

Run	Catalyst	Loading[b] [wt%]	T [°C]	Conversion [%]	Yield[c] [%] Sor	Man	Glu	Gly+EG
1	Ru	3.2	140	100	72.9	1.2	–	7.5
2	Ru	3.2	150	100	**95.1**	2.0	–	1.3
3	Ru	3.2	155	100	89.9	2.0	–	0.4
4	Ru	3.2	160	100	80.8	2.8	–	1.2
5	Ru	1.2	150	92.5	23.4	0.7	3.2	–
6	Ru	3.2	150	100	**95.1**	2.0	–	1.3
7	Ru	3.7	150	100	92.8	2.7	–	1.9
8	Ru	4.6	150	100	85.4	3.2	–	1.0
9	Ru	5.8	150	100	77.8	3.6	–	0.6
10	Ru	8.0	150	100	3.8	1.2	–	0.9
11[d]	MIL-100(Cr)	–	190	33.2	–	–	13.5	7.2
12[d]	PTA/MIL-100(Cr)	16.7	190	41.4	–	–	11.3	5.6
13[d]	Ru/MIL-100(Cr)	3.2	190	100	56.0	3.8	–	5.0

[a] Reaction conditions: cellobiose (50 mg), Ru-PTA/MIL-100(Cr) (30 mg, 16.7 wt% PTA), water (5.0 mL), 140–160 °C, hydrogen pressure of 2.0 MPa, 10 h. [b] Ru loadings of the catalyst were determined by ICP–OES analysis. [c] Sor, Man, Glu, and Gly denote sorbitol, mannitol, glucose, and glycerol, respectively; Gly+EG indicates combined yield of Gly and EG. [d] Blank experiments.

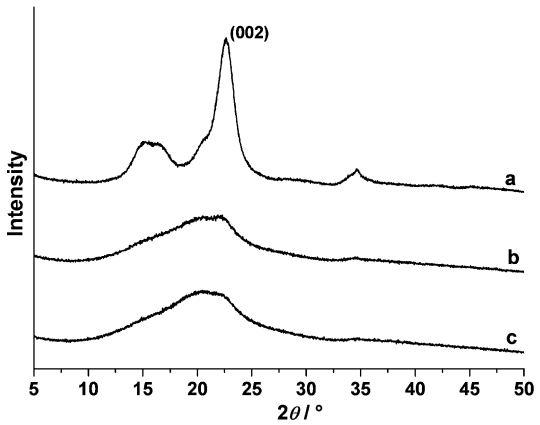

Figure 2. XRD patterns of ball-millled cellulose: a) nontreated and milled for b) 2000 and c) 3000 min.

CrI of cellulose significantly decreased during pretreatment (ball millling), but further pretreatment (>3000 min) did not result in a clear improvement.

FTIR spectra (Figure 3) demonstrate the changes in the main structure of cellulose after ball milling. The band at 1430 cm^{-1}, corresponding to CH_2 scissoring motions in cellulose I crystals, was strong for commercial cellulose, but became weaker and

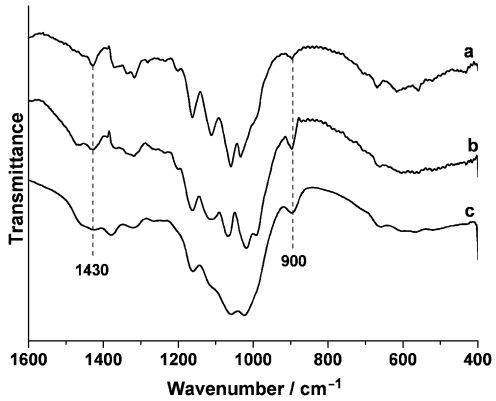

Figure 3. FTIR spectra of ball-milled cellulose: a) nontreated and milled for b) 2000 and c) 3000 min.

broader after ball milling, indicating a conformational change of CH_2OH at the C6 position (from a regular arrangement to a random one).[49] In addition, the bands at around 1320–1376 and 1032–1165 cm^{-1}, which were assigned to various C–H and C–O groups on the glucose anhydride ring, deformed and smoothed gradually after ball milling. However, the band at 900 cm^{-1}, arising from C–O–C vibrations of β-glycosidic linkages, was almost unchanged, suggesting that C–O–C bonds of β-glucosides remained intact in all treated samples. FTIR results for these samples further confirmed that the crystallinity of cellulose was significantly reduced after ball milling, whereas most β-glucoside structures in the cellulose molecule were sustained.[13] We thus compared nontreated and ball-milled cellulose as far as further conversion of cellulose into sorbitol was concerned.

The influence of cellulose crystallinity on cellulose conversion into sorbitol was investigated. For this purpose, the reactivity of cellulose with or without pretreatment was compared in hydrolytic hydrogenation reactions. Sorbitol yields of 17.7% with a cellulose conversion of 55.6% were obtained from nontreated cellulose (CrI = 75%) with Ru-PTA/MIL-100(Cr) as the catalyst (Table 2, run 1). In contrast, cellulose that had been milled for 2000 min (CrI = 16%) was completely converted with

Table 2. Effect of cellulose pretreatment (ball-milling) time and reaction time on cellulose conversion into sorbitol.[a]

Run	Ball-milling time [min]	Reaction time [h]	Conversion [%]	Yield[b] [%] Sor	Man	Glu	Gly+EG
1[c]	–	10.0	55.6	**17.7**	2.4	–	1.0
2[d]	2000	8.0	100	47.2	5.8	0.1	2.0
3	2000	10.0	100	**49.0**	6.6	–	6.5
4	2000	12.0	100	15.3	3.4	–	2.5
5[e]	3000	7.0	100	53.0	4.7	–	4.5
6	3000	8.0	100	**57.9**	5.3	–	1.0
7	3000	8.5	100	54.6	5.0	0.1	3.4
8	3000	9.0	100	51.9	4.8	–	1.1
9	3000	10.0	100	45.8	5.4	–	1.0

[a] Reaction conditions: cellulose (50 mg), Ru-PTA/MIL-100(Cr) (30 mg, 3.2 wt% Ru, 16.7 wt% PTA), water (8.0 mL), 190 °C, hydrogen pressure of 2.0 MPa. [b] Sor, Man, Glu, and Gly denote sorbitol, mannitol, glucose, and glycerol, respectively; Gly+EG indicates combined yield of Gly and EG.

a sorbitol yield of 49.0% (Table 1, run 3). Surprisingly, for cellulose that had been milled for 3000 min (CrI = 10%), both excellent sorbitol yields of 57.9% and a conversion of 100% were achieved (Table 1, run 6). Furthermore, the main products were C6 sugar alcohols (sorbitol and mannitol) with yields of up to 63.2% obtained from cellulose that had been milled for 3000 min, whereas no glucose could be detected, emphasizing the high hydrogenation activity of catalyst Ru-PTA/MIL-100(Cr). Moreover, due to the fact that the hydrolysis of cellulose is the rate-determining step in the conversion of cellulose into sorbitol, a complete conversion within 8 h suggests a high hydrolysis activity of PTA/MIL-100(Cr) towards pretreated cellulose. In contrast, for nontreated cellulose reaction times of 10 h are requisite to obtain a conversion of only 55.6% (Table 2, run 1). Other identified products during the hydrolytic hydrogenation of cellulose were mannitol, glycerol, and EG under the above reaction conditions (Table 2, run 1).

Sorbitol yields increased with reaction time to a maximum of 49.0% after 10 h for cellulose that had been milled for 2000 min (Table 2, runs 2–4), and 57.9% after 8 h for cellulose that had been milled for 3000 min (Table 2, runs 5–9). For longer reaction times, sorbitol yields decreased, although ball-milled cellulose conversions approached 100%. The improved sorbitol yields and reduced reaction times for pretreated cellulose thus indicate that reduction of the cellulose CrI through ball milling can efficiently enhance its reactivity.

Table 3. Effect of reaction temperature and hydrogen pressure on cellulose conversion into sorbitol.[a]

Run	P_{H_2} [MPa]	T [°C]	Conversion [%]	Yield[b] [%] Sor	Man	Glu	Gly+EG
1	2.0	180	76.1	34.5	3.9	0.1	1.1
2	2.0	185	88.6	42.5	4.8	–	0.3
3	2.0	190	100	**49.0**	6.6	–	6.5
4	2.0	195	100	45.4	6.5	0.2	0.6
5	2.0	200	100	17.5	4.4	0.5	3.2
6	–[c]	190	85.5	–	–	–	4.9
7	0.5	190	93.4	9.9	1.5	0.7	4.0
8	1.0	190	95.3	44.7	5.0	0.2	1.8
9	2.0	190	100	**49.0**	6.6	–	6.5
10	3.0	190	100	45.8	4.1	–	0.4
11	5.0	190	100	42.3	5.1	0.2	1.6

[a] Reaction conditions: cellulose ball-milled for 2000 min (50 mg), Ru-PTA/MIL-100(Cr) (30 mg, 3.2 wt% Ru, 16.7 wt% PTA), water (8 mL), 180–200 °C, hydrogen pressure of 0.5–5.0 MPa. [b] Sor, Man, Glu, and Gly denote sorbitol, mannitol, glucose, and glycerol, respectively; Gly+EG indicates combined yield of Gly and EG. [c] 2 MPa N_2 instead of H_2.

The effects of reaction temperature and hydrogen pressure on cellulose conversion into sorbitol were also investigated (Table 3). Cellulose conversion increased as the temperature increased, but sorbitol yield reached a maximum of 49.0% at 190 °C. A further increase in temperature to 200 °C, however, led to a slight reduction in sorbitol yields to 45.4%, which was presumably due to acid-catalyzed sorbitol degradation under higher reaction temperatures (Table 3, runs 1–5). Thus, the effect of reaction temperature on cellulose conversion was in accordance with that of cellobiose. It was also found that hydrogen played a crucial role in the conversion of cellulose. In the absence of H_2 (under N_2 at 2 MPa), cellulose conversion was 85.5%; however, glucose, the expected cellulose hydrolysis product, was not detected due to a PTA/MIL-100(Cr) solid-acid-catalyzed degradation reaction of glucose under high temperatures (Table 3, run 6). The increase in H_2 pressure significantly increased cellulose conversion up to 100%, but sorbitol yields reached a maximum of 49.0% at 2.0 MPa (Table 3, run 6–11). This result was presumably attributed to competitive adsorption between H_2, cellulose, and glucose on the surface of Ru-PTA/MIL-100(Cr). An increase in H_2 pressure would possibly lead to a decreased adsorption of both cellulose and glucose, which would accordingly result in a slow formation of glucose and sorbitol, respectively. Because both hydrogenation and hydrogenolysis are competitive surface reactions[28] on Ru-PTA/MIL-100(Cr), hydrogenolysis of the subsequently produced sorbitol would dominate if glucose was supplied too slowly, which would further lead to decreased sorbitol yields beyond an optimized H_2 pressure.

It is expected that Ru-PTA/MIL-100(Cr) with a controllable amount and strength of acid sites in the support PTA/MIL-100(Cr) is an ideal model to investigate the balance between the amount and strength of acid sites and the activity of metallic sites for the hydrogenation in cellulose conversion into sorbitol. The control of encapsulated-PTA loading in MIL-100(Cr) was performed by adding different quantities of PTA to the synthesis solution of MIL-100(Cr), which resulted in variable encapsulated-PTA loadings in PTA/MIL-100(Cr).[44] It is assumed that tungsten is only present in PTA molecules (one PTA molecule contains twelve tungsten atoms) and chromium exists only in MOF form. The precise PTA loading levels in PTA/MIL-100(Cr) were determined by performing inductively coupled plasma optical emission spectroscopy (ICP–OES), whereas the total amount and strength of acid sites in PTA/MIL-100(Cr) was determined by using a combination of apparent pH and acid-density measurements of PTA/MIL-100(Cr). Thus, encapsulated-PTA loadings in MIL-100(Cr) range from 8.3 (W/Cr molar ratio of 0.1) to 24.2 wt% (W/Cr molar ratio of 0.4) corresponding to the apparent pH of PTA/MIL-100(Cr) (from 3.72 to 3.52) and the acid site density of PTA/MIL-100(Cr) (from 2.59 to 4.22 mmol g^{-1}) under the above preparation conditions (Table 4, runs 2–4). Furthermore, the acid strength of PTA/MIL-100(Cr) increases with the increase in PTA concentration in PTA/MIL-100(Cr). These results confirm that the control of encapsulated-PTA loadings in MIL-100(Cr) is possible.

Table 4. Composition and acid strength of POM/MIL-100(Cr).

Run	Support	POM loading [mM]	POM loading [wt%][a]	Cr[a] [wt%]	W/Mo[a] [wt%]	W/Cr[a] [%]	pH[b]	Acid density[c] [mmol g^{-1}]
1	MIL-100(Cr)	–	–	–	–	–	3.91	1.39
2	PTA/MIL-100(Cr)	0.3	8.3	16.1	6.4	0.1	3.72	2.59
3	PTA/MIL-100(Cr)	0.6	16.7	14.0	12.8	0.3	3.70	3.36
4	PTA/MIL-100(Cr)	0.9	24.2	11.8	18.6	0.4	3.52	4.22
5	STA/MIL-100(Cr)	0.6	23.3	13.1	17.8	0.4	3.90	2.53
6	PMA/MIL-100(Cr)	1.0	17.1	15.6	10.8[d]	0.4[e]	3.50	3.61

[a] Based on ICP-OES analysis. [b] Apparent pH values were generated by suspending corresponding MOFs (30 mg) in an aqueous solution of KCl (20 mL, 10 mM). [c] Acid-density values were determined through acid–base titration and calculated using the amount of NaOH added to the corresponding MOF material. [d] Mo. [e] Mo/Cr.

Furthermore, in the cases of silicotungstic acid (STA) and phosphomolybdic acid (PMA) encapsulated in MIL-100(Cr) [denoted as STA/MIL-100(Cr) and PMA/MIL-100(Cr), respectively], the composition and acid strength of MIL-100(Cr), STA/MIL-100(Cr), and PMA/MIL-100(Cr) were also defined using the same methods as those shown in Table 4 (runs 1, 5–6). Therefore, the acid site density of these POM/MOF hybrid materials decreased in the order: PTA/MIL-100(Cr) (24.2 wt% PTA) > PMA/MIL-100(Cr) (17.1 wt% PMA) > PTA/MIL-100(Cr) (16.7 wt% PTA) > PTA/MIL-100(Cr) (8.3 wt% PTA) > STA/MIL-100(Cr) (23.3 wt% STA) > MIL-100(Cr), which was also in agreement with the acid-strength sequence obtained from apparent pH measurements.

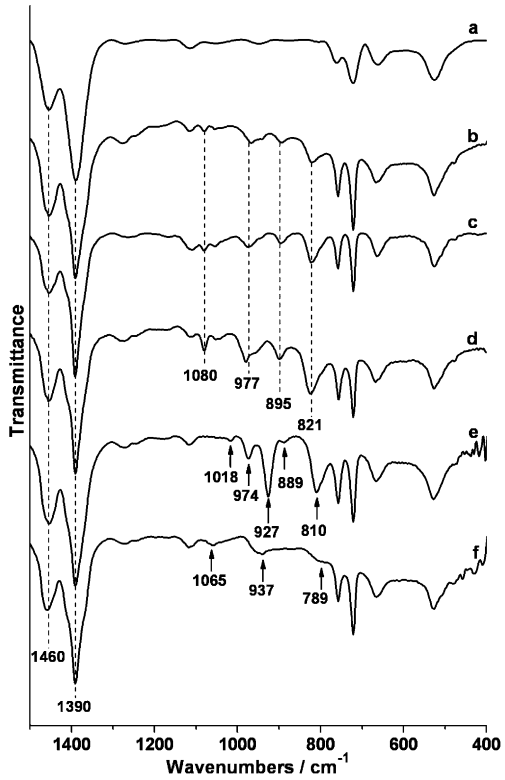

Figure 4. FTIR spectra of a) MIL-100(Cr), b) PTA/MIL-100(Cr) (8.3 wt% PTA), c) PTA/MIL-100(Cr) (16.7 wt% PTA), d) PTA/MIL-100(Cr) (24.2 wt% PTA), e) STA/MIL-100(Cr) (23.3 wt% STA), and f) PMA/MIL-100(Cr) (17.1 wt% PMA).

FTIR spectra of MIL-100(Cr), PTA/MIL-100(Cr), STA/MIL-100(Cr), and PMA/MIL-100(Cr) were compared (Figure 4). The IR spectrum of a typical MIL-100(Cr) sample clearly showed the presence of vibrational bands characteristic of framework –(O–C–O)– groups at around 1390 and 1460 cm^{-1}, confirming the coordination of the tricarboxylate within the MIL-100(Cr) framework (Figure 4a).[45]

According to literature, crystalline PTA shows characteristic bands at 1080 (vibrational frequency of P–O_a), 978 (stretching of W=O_d), 888 (vibrational frequency of W–O_b–W), and 815 cm^{-1} (W–O_c–W vibration).[50] In the case of PTA/MIL-100(Cr) with a PTA concentration of 8.3–24.2 wt% all characteristic stretching bands of PTA are present in the PTA/MIL-100(Cr) spectra (Figure 4b–d). The characteristic bands corresponding to P–O_a vibrations of PTA/MIL-100(Cr) are perfectly visible at 1080 cm^{-1}, in accordance with the literature. In addition, vibrations corresponding to the stretching of W=O_d bonds appear at 977 cm^{-1}. Vibrations that are associated with W–O_b–W and W–O_c–W bonds are observed at 895 and 821 cm^{-1}, respectively (Figure 4b–d). Relative to experimental spectra of PTA, these vibrations from PTA/MIL-100(Cr) are upshifted by 6–7 cm^{-1} due to interactions with the surface of MIL-100(Cr).[44] Furthermore, the intensity of PTA signals [relative to MIL-100(Cr) signals] increased with the increase in PTA concentration from 8.3 to 24.2 wt% in PTA/MIL-100(Cr) (Figure 4b–d).

The FTIR spectra of STA/MIL-100(Cr) contain typical bands belonging to STA with Keggin structures. The bands at 1018 and 927 cm^{-1} are assigned to stretching vibrations of Si–O_a, whereas the peak at 974 cm^{-1} can be indexed to terminal band vibrations of W=O_d. Vibrations that are associated with W–O_b–W and W–O_c–W are observed at 889 and 810 cm^{-1}, respectively (Figure 4e).[50,51] In the case of PMA/MIL-100(Cr), the peaks at 1065 and 937 cm^{-1} can be assigned to stretching vibrations of P–O_a and terminal band vibrations of Mo=O_d, respectively, whereas the band at 789 cm^{-1} is associated with Mo–O_c–Mo (Figure 4f). The unobserved peak at 873 cm^{-1}, associated with stretching vibrations of Mo–O_b–Mo, is presumably covered by framework bands of MIL-100(Cr).[50,51] The above FTIR spectra analysis thus further indicates that POMs, including PTA, STA, and PMA, were successfully encapsulated in MIL-100(Cr).

To further probe the acid strength and respective roles of PTA in sorbitol formation, different weight ratios of PTA were employed for Ru-PTA/MIL-100(Cr), whereas loading amounts of Ru were kept constant (Table 5). The activity of catalyst Ru-PTA/MIL-100(Cr) increased with increasing PTA loadings; maximum sorbitol yields of 49.0% were observed at a PTA loading of 16.7 wt% (Table 5, run 1–3). A further increase in PTA loading to 24.2 wt%, however, led to a slightly reduced sorbitol yield of 48.7% (Table 5, run 3). Such behavior may be

Table 5. Effect of catalyst composition [M-POM/MIL-100(Cr)] on cellulose conversion into sorbitol.[a]

Run	M		POM		Conversion	Yield[b] [%]			
	metal	loading [wt%]	material	loading [wt%]	[%]	Sor	Man	Glu	Gly+EG
1	Ru	3.2	PTA	8.3	86.6	34.0	6.5	–	0.4
2	Ru	3.2	PTA	16.7	100	**49.0**	6.6	–	6.5
3	Ru	3.2	PTA	24.2	100	48.7	4.9	–	1.0
4	Ru	3.2	STA	23.3	100	27.6	10.6	–	–
5	Ru	3.2	PMA	17.1	100	11.2	4.1	1.0	9.0
6	Ru	1.2	PTA	16.7	78.2	23.0	2.8	1.1	3.0
7	Ru	3.7	PTA	16.7	100	47.5	5.9	0.2	0.4
8	Ru	4.6	PTA	16.7	100	40.7	7.5	0.1	0.7
9	Ru	5.8	PTA	16.7	100	28.1	7.1	1.2	0.7
10	Ru	8.0	PTA	16.7	100	18.1	6.8	0.2	1.8
11	Pt	2.8	PTA	16.7	100	16.7	1.1	3.0	0.7
12	Rh	2.8	PTA	16.7	100	3.8	1.3	2.7	5.4
13	Pd	2.3	PTA	16.7	79.6	3.3	0.6	4.3	3.7
14[c]	MIL-100(Cr)		–	–	46.3	–	–	0.5	4.1
15[c]	PTA/MIL-100(Cr)		PTA	16.7	58.1	–	–	0.8	8.5
16[c]	Ru/MIL-100(Cr)		Ru	3.2	100	13.5	9.9	0.3	6.3

[a] Reaction conditions: cellulose ball milled for 2000 min (50 mg), M-MOF/MIL-100(Cr) (30 mg; M = Ru, Rh, Pd, Pt; POM = PTA, STA, PMA; runs 1–13), water (8.0 mL), 190 °C, hydrogen pressure of 2.0 MPa, 10 h. [b] Sor, Man, Glu, and Gly denote sorbitol, mannitol, glucose, and glycerol, respectively. Gly+EG indicates combined yield of Gly and EG. [c] Blank experiments.

explained as a result of the increase in the acid strength of PTA/MIL-100(Cr) on the one hand and the decrease in the surface area of PTA/MIL-100(Cr) on the other hand as PTA loadings increase. Due to the fact that glucose hydrogenation to sorbitol occurs through a surface-type catalysis,[28] decreasing the surface area of the catalyst would presumably result in decreased sorbitol yields. Additionally, with Ru-PTA/MIL-100(Cr) (24.2 wt% PTA) as the catalyst, a further dehydration of sorbitol to sorbitan and isosorbide was also observed, suggesting a strong acidity of Ru-PTA/MIL-100(Cr) with high PTA loadings, which may also result in decreased sorbitol yields.

Apart from PTA/MIL-100(Cr), both STA/MIL-100(Cr) and PMA/MIL-100(Cr) were also evaluated as supports to investigate the effect of POMs on cellulose conversion. Both Ru-STA/MIL-100(Cr) and Ru-PMA/MIL-100(Cr) resulted in relatively low sorbitol yields of 27.6% and 11.2%, respectively, under the same reaction conditions (Table 5, runs 4 and 5). Therefore, Ru-PTA/MIL-100(Cr) (3.2 wt% Ru, 16.7 wt% PTA) was considerably more active and selective (in terms of sorbitol formation) than Ru-STA/MIL-100(Cr) and Ru-PMA/MIL-100(Cr) (Table 5, runs 1–5). Zhang et al. discussed the effect of W in supported tungsten carbide and bimetallic catalysts:[29–31] high conversions and a shift in selectivity to EG in the presence of W during cellulose conversion into EG were observed. Furthermore, Palkovits et al. revealed a cooperative effect between W and Ru for the dual functional catalyst system Ru/C and PTA during the conversion of cellulose into sugar alcohols.[27] Considering selectivities of up to 63.2% for C_6 sugar alcohols (sorbitol and mannitol) over Ru-PTA/MIL-100(Cr) (Table 2, run 6), in principle our results seemed to agree with the above proposition: the presence of W enhances the selectivity for certain products, a fact which may be attributed to cooperative effects between tungsten, ruthenium, and the substrate. Thus, the differences in product selectivity between STA, PMA, and PTA could originate from differences in their interaction with the substrate and ruthenium. Further investigations will be carried out to elucidate underlying principles. Therefore, with a constant Ru loading, the catalytic performance of Ru-POM/
MIL-100(Cr) decreased in the order: Ru-PTA/MIL-100(Cr) (16.7 wt% PTA) > Ru-PTA/MIL-100(Cr) (24.2 wt% PTA) > Ru-PTA/MIL-100(Cr) (8.3 wt% PTA) > Ru-STA/MIL-100(Cr) (23.3 wt% STA) > Ru-PMA/MIL-100(Cr) (17.1 wt% PMA). The above results are, however, quite different from the acid-strength sequence of the support POM/MIL-100(Cr) shown in Table 4, which further indicates the delicate balance between acid strength, surface area, and metal of catalyst.

Notably, PMA/MIL-100(Cr) showed a relatively high acid strength (Table 4), whereas Ru-PMA/MIL-100(Cr) had the lowest yield in sorbitol (Table 5, runs 1–5). Previous studies indicate that the rate of cellulose hydrolysis is strongly dependent on acid concentration.[52] The catalytic activity of heteropolyacids, both in homogeneous and heterogeneous systems, usually parallels their acid strength (PTA > STA > PMA).[50,51] Being a stronger acid and, therefore, a more efficient proton donor, PTA usually exhibits higher catalytic activities than other heteropolyacid catalysts. Furthermore, the hydrolysis rate of cellulose is generally controlled by the catalyst acid strength, and therefore, Ru-PTA/MIL-100(Cr) shows the highest catalytic activity in the Ru-POM/MIL-100(Cr) series. In the case of Ru-PMA/MIL-100(Cr), because of the relatively lower thermal stability, higher oxidation potential, and lower hydrolytic stability of PMA relative to tungsten heteropolyacids,[50,51] molybdenum heteropolyacids are frequently deactivated due to their reduction by the organic reaction medium; it is not uncommon for them to show lower activities than those expected from their acid strengths.[50,51] Accordingly, on the basis of a combination of acid strength and stability of catalyst, catalyst efficiency in the hydrolytic hydrogenation of cellulose decreases in the order: Ru-PTA/MIL-100(Cr) > Ru-STA/MIL-100(Cr) > Ru-PMA/MIL-100(Cr) (Table 5, runs 1–5).

Different amounts of Ru were loaded on the PTA/MIL-100(Cr) (16.7 wt% PTA) support, and the effect of Ru loadings on sorbitol yields was also studied (Table 5, runs 2, 6–10). The use of Ru-PTA/MIL-100(Cr) with a Ru loading of 1.2 wt% produced sorbitol in 23.0% yield with a cellulose conversion of 78.2%. Furthermore, a combined analysis of data from different loading amounts suggested that Ru-PTA/MIL-100(Cr) with a Ru and PTA loading of 3.2 and 16.7 wt%, respectively, showed the highest sorbitol yield and the highest selectivity for sorbitol. These results were in agreement with the Ru loading effect on the hydrolytic hydrogenation of cellobiose.

Furthermore, data in Table 1 (runs 2, 11–13) and Table 5 (runs 2, 14–16) revealed that ruthenium significantly promoted cellobiose and cellulose conversion. However, the acid site density of Ru/MIL-100(Cr) (1.62 mmol g^{-1}) and Ru-PTA/MIL-100(Cr) (3.53 mmol g^{-1}) only increased slightly relative to their corresponding supports (Table 4, runs 1 and 3). The increase in cellobiose and cellulose conversion thus can presumably be related to hydrolytic hydrogenation and hydrogenolysis processes of cellobiose and cellulose catalyzed by the ruthenium catalyst. As a result, both sorbitol, formed by a hydrolytic hydrogenation process, and 3-β-gluco-pyranosyl-D-glucitol,[10,14,24] generated through a hydrogenolysis process, were observed in the metal-catalyzed reaction.

Fukuoka et al. reported that both supported Pt and Ru catalysts were effective for the conversion of cellulose into sugar alcohols.[11,15] In our case, relative to Pt, Rh, and Pd, supported Ru was more active and selective for the formation of sorbitol, and Ru-PTA/MIL-100(Cr) resulted in the highest yield in sorbitol among the examined catalysts (Table 5, runs 2, 11–13). Additionally, both supports MIL-100(Cr) and PTA/MIL-100(Cr) were used as catalysts in blank experiments for cellulose conversion into sorbitol. No sugar alcohols were observed and only trace amounts of glucose were detected by hydrolysis of cellulose with MIL-100(Cr) and PTA/MIL-100(Cr) as a Lewis acid and a Brønsted acid, respectively, under the above conditions (Table 5, runs 14 and 15). Using Ru/MIL-100(Cr) as a catalyst, a low sorbitol yield of 13.5% was observed, which was in sharp contrast with Ru-PTA/MIL-100(Cr) producing sorbitol yields of 49.0% (Table 5, runs 16 and 2, respectively). These results demonstrated that a good balance between the two cata-

lytic functions of the transition-metal catalyst and the acid strength of the solid support material is important.

Catalyst recycling

The reusability of catalyst Ru-PTA/MIL-100(Cr) was evaluated for the hydrolytic hydrogenation of cellobiose. The catalyst was recovered and reused directly for the next run under the same conditions as those described in Table 1 (run 2). However, the observed sorbitol yield was sharply decreased to 8.5% with the recovered catalyst, which is far inferior to that of the freshly prepared catalyst, producing sorbitol in 95.1% yield (Table 1, run 2). ICP–OES analysis showed that only 0.006%, 0.005%, and 0.003% of the total amount of Cr, W, and Ru, respectively, had leached from Ru-PTA/MIL-100(Cr) after the first run. The reason for catalyst deactivation thus can hardly be related to the leaching of active species from the catalyst. One important reason maybe that some insoluble substances, such as oligomeric products, were absorbed on the highly porous solid catalyst and poisoned the catalyst, leading to low sorbitol yields.[53,54]

Evaluation of the catalyst acid/metal balance

According to the related methodology available on the evaluation of acid–metal bifunctional catalysts,[26,55] the experimental data set thus far obtained has been used to rationalize the acid/metal balance requirements of Ru-PTA/MIL-100(Cr) for the hydrolytic hydrogenation of cellobiose and cellulose to hexitols (sorbitol and mannitol). Taking the characterization results reported in Tables 1, 4, and 5 into account, the ratio of acid site density to the number of Ru surface atoms (n_A/n_{Ru}) was used to monitor the balance between the hydrolysis and hydrogenation functions. Due to the fact that both sorbitol and mannitol are hydrolytic hydrogenation products of cellobiose and cellulose, Figure 5 shows the relationship between n_A/n_{Ru} and corresponding hexitol yields. Considering the inevitable experimental error in this type of complicated reactions, the observed relationship appears to be relatively good.

A lower value of n_A/n_{Ru} (<8.84) indicates a lower n_A or a relatively higher n_{Ru} value. As both hydrogenation and hydrogenolysis are competitive surface reactions[28] on Ru-PTA/MIL-100(Cr), a decrease in acid strength accordingly results in a slow formation of glucose; conversely, an increase in the number of metallic sites leads to a high hydrogenation rate of glucose to afford sorbitol. However, hydrogenolysis of subsequently produced sorbitol dominates if glucose is supplied slowly, which will further lead to a decreased yield in sorbitol. The above discussion thus reveals that a lower value of n_A/n_{Ru} (<8.84), arising from either low acid strength or high loading amounts of Ru, leads to a reduced yield in hexitol suggesting the further need for an increased number of acid sites in Ru-PTA/MIL-100(Cr) for the catalytic depolymerization of cellobiose and cellulose and other subsequent hydrolysis reactions. When the acid site density is high enough to establish a proper balance between the two catalytic functions ($8.84<n_A/n_{Ru}<12.90$), hexitol yields reach a maximum of nearly 97.1% from cellobiose and 55.6% from cellulose.

For increasingly higher values of this ratio achieved by increasing the acid site density of catalyst Ru-PTA/MIL-100(Cr), it is more likely that glucose is subjected to another acid-catalyzed degradation reaction rather than being hydrogenated to hexitols. In addition, a further dehydration of sorbitol to sorbitan and isosorbide was also observed, suggesting a strong acidity of Ru-PTA/MIL-100(Cr) with a high n_A/n_{Ru} ratio, which is another reason leading to a decreased sorbitol yield. On the other hand, when higher n_A/n_{Ru} values arise from a decrease in n_{Ru}, the lower loading amount of Ru will thus be insufficient to fully hydrogenate the intermediate glucose into sorbitol, which will also result in a decreased sorbitol yield.

Characterization of supported Ru catalysts

To identify the active species for hydrogenation, XRD analysis was performed for Ru-PTA/MIL-100(Cr). Figure 6 represents the XRD patterns of PTA/MIL-100(Cr), Ru-PTA/MIL-100(Cr), and the differential pattern of Ru-PTA/MIL-100(Cr) minus PTA/MIL-100(Cr). The diffraction patterns of PTA/MIL-100(Cr) are assigned to a MTN (a zeolite-type structure, see the Atlas of Zeo-

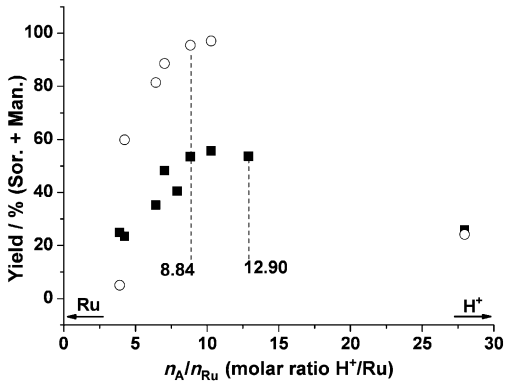

Figure 5. Relationship between the n_A/n_{Ru} (H^+/Ru) ratio and observed hexitol (sorbitol and mannitol) yields for cellobiose (○) and cellulose (■) conversions catalyzed by Ru-PTA/MIL-100(Cr).

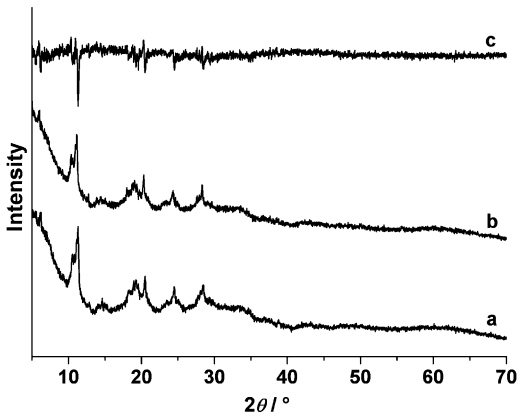

Figure 6. XRD patterns of a) PTA/MIL-100(Cr), b) Ru-PTA/MIL-100(Cr), and c) differential pattern of (b)–(a).

lites) topology and no differences are observed between PTA/MIL-100(Cr) and MIL-100(Cr) according to literature data.[44] Furthermore, there is no observable presence of PTA diffraction lines in PTA/MIL-100(Cr), suggesting a good dispersion of PTA throughout PTA/MIL-100(Cr). However, after the loading of Ru, no diffraction peaks corresponding to Ru appeared in the XRD patterns of Ru-PTA/MIL-100(Cr), which indicates that highly dispersed Ru species exist in small nanoparticles or in amorphous structures.

The typical TEM micrograph and the particle-size distribution of Ru nanoparticles on PTA/MIL-100(Cr) are shown in Figure 7, demonstrating that the mean diameter of highly dispersed Ru nanoparticles was 1.4 nm with a narrow distribution. These results further confirm the results of the XRD patterns.

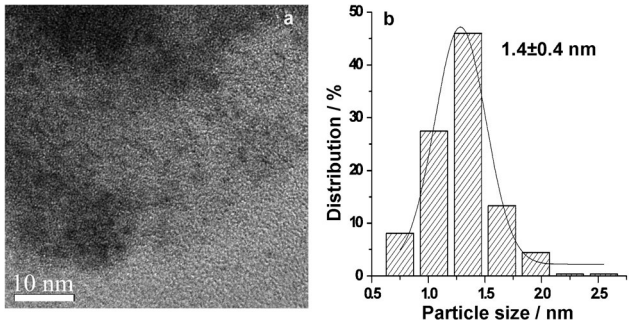

Figure 7. TEM micrographs (a) and size distribution (b) of Ru-PTA/MIL-100(Cr) (3.2 wt% Ru, 16.7 wt% PTA).

Conclusions

We designed a series of elegant POM/MOF-hybrid-supported Ru bifunctional catalysts for the conversion of cellobiose and cellulose into sorbitol in neutral water in the presence of H_2 under relatively mild conditions. Yields in sorbitol of 95.1% and 57.9% can be achieved in the conversion of cellobiose and ball-milled cellulose, respectively. The decrease in the crystallinity of cellulose can promote the formation of sorbitol. Both the type and acid strength of POMs encapsulated in MIL-100(Cr) play a key role in the conversion of cellulose into sorbitol over the present catalyst. The evaluation of an optimum balance between the hydrogenation and hydrolysis functions of the catalysts reveals that a ratio of acid site density to the number of metal surface atoms between 8.84 and 12.90 achieves a maximum conversion of cellulose and cellobiose into hexitol. The catalytic results presented herein not only provide insights into the optimal conditions for the preparation of the bifunctional catalyst Ru-PTA/MIL-100(Cr), but also constitute a diagnostic tool to evaluate the delicate balance between the hydrogenation and hydrolysis functions. New possiblities for the rational design of acid–metal bifunctional catalysts for biomass conversion is thus opened.

Experimental Section

Materials: Unless otherwise stated, all chemicals in this work were commercially available and used without further purification. Ruthenium(III) chloride, potassium tetrachloropalladate(II), chloroplatinic acid(IV), and rhodium(III) chloride were provided by Shanghai Jiu Ling Chemical Co., Ltd. (Shanghai, PR China). Chromium(VI) oxide, benzene-1,3,5-tricarboxylic acid (H_3BTC), hydrofluoric acid (40%), PTA, STA, PMA, D-(+)-cellobiose (98%), and cellulose (microcrystalline, 25 μm) were purchased from Aladdin Industrial Inc. (Shanghai, P.R. China) and Sinopharm Chemical Reagent Co, Ltd. (Shanghai, P.R. China). Cellulose was pretreated using a ball mill (NanDa Instrument, QM-3SP04). Cellulose was charged in a rotary agate container with agate balls. The container was rotated at a speed of 500 rpm for 2000 or 3000 min.

Characterization techniques: HPLC analyses were performed by using a Shimadzu LC-20AT instrument equipped with a refractive index detector and a Shodex Sugar SP-0810 column (ø: 8× 300 mm; column temperature: 80 °C; mobile phase: water; flow rate: 0.5 mL min^{-1}). High-resolution TEM (HRTEM) was recorded by using a JEM-2010HR instrument at 20 keV. IR spectra were measured by using a Bruker Tensor 27 FTIR spectrometer as KBr pellets. XRD patterns were obtained using a PANalytical X'pert Pro multipurpose diffractometer operated at 40 KV and 40 mA, using Ni-filtered CuK_α radiation. ICP–OES was performed by means of a Perkin–Elmer Optima 8000 instrument. The samples were digested in H_2SO_4 (70%) at 120 °C and then aqua regia was added to the mixture to digest the noble metal. The apparent pH of MOFs was measured using a Leici PHS-25 pH meter. Acid–base titration was performed by using a Metrohm 877 Titrino plus instrument.

Preparation of support and catalysts

MIL-100(Cr): MIL-100(Cr) was prepared according to a literature procedure.[56] Benzene-1,3,5-tricarboxylic acid (H_3BTC, 2.625 g, 12.5 mmol), a hydrofluorohydric solution (0.45 mL, 40%), and 60 mL of deionized water were added to chromium(VI) oxide (CrO_3, 1.25 g, 12.5 mmol) and stirred for a few minutes at room temperature. The mixture was then sealed in a Teflon-lined stainless-steel autoclave (100 mL) and heated at 220 °C for 4 d, followed by slow cooling to room temperature at a rate of 13 °C h^{-1}. The resulting green solid was washed with deionized water and acetone and dried at 70 °C under an air atmosphere.

PTA/MIL-100(Cr): The one-pot synthesis of PTA encapsulated in MIL-100(Cr) was performed by adding three different quantities of PTA (0.9, 1.8, and 3.6 g) to the aforementioned synthesis solution.[43] Then, syntheses were performed as explained above to yield PTA/MIL-100(Cr) (W/Cr molar ratio of 0.1, 0.3, and 0.4, respectively).

STA/MIL-100(Cr) and PMA/MIL-100(Cr): One-pot syntheses of STA and PMA encapsulated in MIL-100(Cr) were performed by using the same procedure as that for PTA/MIL-100(Cr). STA (0.9 g) or PMA (0.9 g) were added to the aforementioned synthesis solution of MIL-100(Cr). Then, syntheses were performed analogously to that of PTA/MIL-100(Cr) to yield STA/MIL-100(Cr) (W/Cr molar ratio of 0.4) or PMA/MIL-100(Cr) (Mo/Cr molar ratio of 0.4), respectively.

Ru-PTA/MIL-100(Cr): Ru-PTA/MIL-100(Cr) (Ru = 3.2 wt%) was prepared by using a conventional impregnation method as follows: PTA/MIL-100(Cr) (300 mg, 16.7 wt% PTA) was dropped into a mixture of $RuCl_3$ (20 mg) and water (3 mL), and the mixture was stirred for 24 h at room temperature. The black solution became green, indicating the adsorption of $RuCl_3$ into the support. After drying

using a rotary evaporator at 80 °C, the solid was treated with H_2 (4 MPa) at 160 °C for 2 h in an autoclave.

Ru-STA/MIL-100(Cr) and Ru-PMA/MIL-100(Cr): Ru-STA/MIL-100(Cr) (3.2 wt% Ru) and Ru-PMA/MIL-100(Cr) (3.2 wt% Ru) were prepared using the same procedure as Ru-PTA/MIL-100(Cr) by a replacement of PTA/MIL-100(Cr) with STA/MIL-100(Cr) (300 mg) or PMA/MIL-100(Cr) (300 mg), respectively.

M-PTA/MIL-100(Cr) (M = Pt, Rh, Pd): M-PTA/MIL-100(Cr) (M = Pt, Rh, Pd) was prepared using the same procedure as Ru-PTA/MIL-100(Cr) by a replacement of $RuCl_3$ (20 mg) with $H_2PtCl_6{\cdot}6H_2O$ (25 mg), $RhCl_3$ (26 mg), or K_2PdCl_4 (30 mg) to yield Pt-PTA/MIL-100(Cr) (2.8 wt% Pt), Rh-PTA/MIL-100(Cr) (2.8 wt% Rh), or Pd-PTA/MIL-100(Cr) (2.3 wt% Pd), respectively.

Cellobiose and cellulose conversion into sorbitol: The conversion of cellobiose and cellulose under H_2 was conducted in a stainless-steel high-pressure reactor (60 mL). Cellobiose (50 mg, 0.29 mmol glucose units) or cellulose (50 mg, 0.31 mmol glucose units), a supported Ru catalyst (30 mg), and water (5 mL for cellobiose and 8 mL for ball-milled cellulose) were charged in the reactor. The reactor was purged with H_2 three times, and then pressurized with H_2 (2.0 MPa) at room temperature prior to heating to the desired reaction temperature (150 °C for cellobiose and 190 °C for cellulose). The reactor was maintained at the desired temperature for 10 h with stirring at 600 rpm. After reaction, the reactor was cooled to room temperature. Products were separated by filtration and decantation, and water-soluble products were analyzed by using a HPLC calibrated for each sugar alcohol and for glucose. Cellulose conversion values were determined by the change in cellulose weight before and after reaction. Solid cellulose separated from the solution phase after the reaction was dried at 80 °C overnight before weight measurement. The yield of polyols was calculated by the equation: yield (%) = $(mol_{C\ in\ products})/(mol_{total;\ C\ in\ reactor}) \times 100\%$.

Acknowledgements

This work was supported by the National Basic Research Program of China (973 Program, 2012CB215304), the 100 Talents Program of the Chinese Academy of Sciences, the International Foundation for Science (F/5203-1), and the Guangdong Natural Science Foundation (S2011010002274).

Keywords: acidity · green chemistry · heterogeneous catalysis · metal–organic frameworks · polyoxometalates

[1] P. Anastas, J. Warner, *Green Chemistry: Theory and Practice*, Oxford University Press, New York, **1998**.
[2] J. N. Chheda, G. W. Huber, J. A. Dumesic, *Angew. Chem.* **2007**, *119*, 7298 – 7318; *Angew. Chem. Int. Ed.* **2007**, *46*, 7164 – 7183.
[3] G. W. Huber, S. Iborra, A. Corma, *Chem. Rev.* **2006**, *106*, 4044 – 4098.
[4] S. van de Vyver, J. Geboers, P. A. Jacobs, B. F. Sels, *ChemCatChem* **2011**, *3*, 82 – 94.
[5] H. Kobayashi, T. Komanoya, S. K. Guha, K. Hara, A. Fukuoka, *Appl. Catal. A* **2011**, *409 – 410*, 13 – 20.
[6] P. L. Dhepe, A. Fukuoka, *Catal. Surv. Asia* **2007**, *11*, 186 – 191.
[7] A. Cabiac, E. Guillon, F. Chambon, C. Pinel, F. Rataboul, N. Essayem, *Appl. Catal. A* **2011**, *402*, 1 – 10.
[8] D. Reyes-Luyanda, J. Flores-Cruz, P. J. Morales-Pérez, L. G. Encarnación-Gómez, F. Y. Shi, P. M. Voyles, N. Cardona-Martínez, *Top Catal.* **2012**, *55*, 148 – 161.
[9] W. P. Deng, Y. L. Wang, Q. H. Zhang, Y. Wang, *Catal. Surv. Asia* **2012**, *16*, 91 – 105.
[10] N. Yan, C. Zhao, C. Luo, P. J. Dyson, H. C. Liu, Y. Kou, *J. Am. Chem. Soc.* **2006**, *128*, 8714 – 8715.
[11] A. Fukuoka, P. L. Dhepe, *Angew. Chem.* **2006**, *118*, 5285 – 5287; *Angew. Chem. Int. Ed.* **2006**, *45*, 5161 – 5163.
[12] C. Luo, S. Wang, H. C. Liu, *Angew. Chem.* **2007**, *119*, 7780 – 7783; *Angew. Chem. Int. Ed.* **2007**, *46*, 7636 – 7639.
[13] W. P. Deng, X. S. Tan, W. H. Fang, Q. H. Zhang, Y. Wang, *Catal. Lett.* **2009**, *133*, 167 – 174.
[14] W. P. Deng, M. Liu, X. S. Tan, Q. H. Zhang, Y. Wang, *J. Catal.* **2010**, *271*, 22 – 32.
[15] H. Kobayashi, Y. Ito, T. Komanoya, Y. Hosaka, P. L. Dhepe, K. Kasai, K. Hara, A. Fukuoka, *Green Chem.* **2011**, *13*, 326 – 333.
[16] H. Kobayashi, H. Matsuhashi, T. Komanoya, K. Hara, A. Fukuoka, *Chem. Commun.* **2011**, *47*, 2366 – 2368.
[17] P. F. Yang, H. Kobayashi, K. Hara, A. Fukuoka, *ChemSusChem* **2012**, *5*, 920 – 926.
[18] A. Shrotri, A. Tanksale, J. N. Beltramini, H. Gurav, S. V. Chilukuri, *Catal. Sci. Technol.* **2012**, *2*, 1852 – 1858.
[19] G. F. Liang, H. Y. Cheng, W. Li, L. M. He, Y. C. Yu, F. Y. Zhao, *Green Chem.* **2012**, *14*, 2146 – 2149.
[20] J. F. Pang, A. Q. Wang, M. Y. Zheng, Y. H. Zhang, Y. Q. Huang, X. W. Chen, T. Zhang, *Green Chem.* **2012**, *14*, 614 – 617.
[21] L. N. Ding, A. Q. Wang, M. Y. Zheng, T. Zhang, *ChemSusChem* **2010**, *3*, 818 – 821.
[22] R. Palkovits, K. Tajvidi, J. Procelewska, R. Rinaldi, A. Ruppert, *Green Chem.* **2010**, *12*, 972 – 978.
[23] S. van de Vyver, J. Geboers, M. Dusselier, H. Schepers, T. Vosch, L. Zhang, G. V. Tendeloo, P. A. Jacobs, B. F. Sels, *ChemSusChem* **2010**, *3*, 698 – 701.
[24] M. Liu, W. P. Deng, Q. H. Zhang, Y. L. Wang, Y. Wang, *Chem. Commun.* **2011**, *47*, 9717 – 9719.
[25] J. W. Han, H. Lee, *Catal. Commun.* **2012**, *19*, 115 – 118.
[26] S. Van de Vyver, J. Geboers, W. Schutyser, M. Dusselier, P. Eloy, E. Dornez, J. W. Seo, C. M. Courtin, E. M. Gaigneaux, P. A. Jacobs, B. F. Sels, *ChemSusChem* **2012**, *5*, 1549 – 1558.
[27] R. Palkovits, K. Tajvidi, A. M. Ruppertc, J. Procelewska, *Chem. Commun.* **2011**, *47*, 576 – 578.
[28] J. Geboers, S. Van de Vyver, K. Carpentier, K. de Blochouse, P. Jacobs, B. Sels, *Chem. Commun.* **2010**, *46*, 3577 – 3579.
[29] N. Ji, M. Y. Zheng, A. Q. Wang, T. Zhang, J. G. Chen, *ChemSusChem* **2012**, *5*, 939 – 944.
[30] M. Y. Zheng, A. Q. Wang, N. Ji, J. F. Pang, X. D. Wang, T. Zhang, *ChemSusChem* **2010**, *3*, 63 – 66.
[31] N. Ji, T. Zhang, M. Y. Zheng, A. Q. Wang, H. Wang, X. D. Wang, J. G. Chen, *Angew. Chem.* **2008**, *120*, 8638 – 8641; *Angew. Chem. Int. Ed.* **2008**, *47*, 8510 – 8513.
[32] A. Corma, G. W. Huber, *Angew. Chem.* **2007**, *119*, 7320 – 7338; *Angew. Chem. Int. Ed.* **2007**, *46*, 7184 – 7201.
[33] R. W. Thring, S. P. R. Katikaneni, N. N. Bakhshi, *Fuel Process. Technol.* **2000**, *62*, 17 – 30.
[34] R. D. Cortright, R. R. Davda, J. A. Dumesic, *Nature* **2002**, *418*, 964 – 967.
[35] G. W. Huber, J. N. Chheda, C. J. Barrett, J. A. Dumesic, *Science* **2005**, *308*, 1446 – 1450.
[36] B. Kamm, *Angew. Chem.* **2007**, *119*, 5146 – 5149; *Angew. Chem. Int. Ed.* **2007**, *46*, 5056 – 5058.
[37] M. Banu, P. Venuvanalingam, R. Shanmugam, B. Viswanathan, S. Sivasanker, *Top. Catal.* **2012**, *55*, 897 – 907.
[38] T. Okuhara, *Chem. Rev.* **2002**, *102*, 3641 – 3666.
[39] K. Shimizu, H. Furukawa, N. Kobayashi, Y. Itaya, A. Satsuma, *Green Chem.* **2009**, *11*, 1627 – 1632.
[40] W. Deng, M. Liu, Q. Zhang, X. Tan, Y. Wang, *Chem. Commun.* **2010**, *46*, 2668 – 2670.
[41] C. Y. Sun, S. X. Liu, D. D. Liang, K. Z. Shao, Y. H. Ren, Z. M. Su, *J. Am. Chem. Soc.* **2009**, *131*, 1883 – 1888.
[42] Y. M. Zhang, V. Degirmenci, C. Li, E. J. M. Hensen, *ChemSusChem* **2011**, *4*, 59 – 64.
[43] L. Bromberg, Y. Diao, H. M. Wu, S. A. Speakman, T. A. Hatton, *Chem. Mater.* **2012**, *24*, 1664 – 1675.
[44] J. Juan-Alcañiz, M. G. Goesten, E. V. Ramos-Fernandez, J. Gascon, F. Kapteijn, *New J. Chem.* **2012**, *36*, 977 – 987.
[45] P. P. Long, H. W. Wu, Q. Zhao, Y. X. Wang, J. X. Dong, J. P. Li, *Microporous Mesoporous Mater.* **2011**, *142*, 489 – 493.

[46] J. L. C. Rowsell, O. M. Yaghi, *Angew. Chem.* **2005**, *117*, 4748 – 4758; *Angew. Chem. Int. Ed.* **2005**, *44*, 4670 – 4679.
[47] A. Fukuoka, P. L. Dhepe, *Chem. Rec.* **2009**, *9*, 224 – 235.
[48] J. A. Geboers, S. Van de Vyver, R. Ooms, B. Op de Beeck, P. A. Jacobs, B. F. Sels, *Catal. Sci. Technol.* **2011**, *1*, 714 – 726.
[49] A. Mihranyan, A. P. Llagostera, R. Karmhag, M. Strømme, R. Ek, *Int. J. Pharm.* **2004**, *269*, 433 – 442.
[50] I. V. Kozhevnikov, *Appl. Catal. A* **2003**, *256*, 3 – 18.
[51] M. N. Timofeeva, *Appl. Catal. A* **2003**, *256*, 19 – 35.
[52] S. Yildiz, E. D. Gezer, U. C. Yildiz, *Build. Environ.* **2006**, *41*, 1762 – 1766.
[53] Z. H. Zhang, K. Dong, Z. B. Zhao, *ChemSusChem* **2011**, *4*, 112 – 118.
[54] Y. Leng, J. Wang, D. R. Zhu, Y. J. Wu, P. P. Zhao, *J. Mol. Catal. A* **2009**, *313*, 1 – 6.
[55] J. W. Thybaut, C. S. Laxmi Narasimhan, J. F. Denayer, G. V. Baron, P. A. Jacobs, J. A. Martens, G. B. Marin, *Ind. Eng. Chem. Res.* **2005**, *44*, 5159 – 5169.
[56] P. L. Llewellyn, S. Bourrelly, C. Serre, A. Vimont, M. Daturi, L. Hamon, G. De Weireld, J.-S. Chang, D.-Y. Hong, Y. K. Hwang, S. H. Jhung, G. Férey, *Langmuir* **2008**, *24*, 7245 – 7250.

Received: November 30, 2012
Revised: February 3, 2013
Published online on ■■ ■■, 0000

J. Chen, S. Wang, J. Huang, L. Chen,* L. Ma, X. Huang*

■■ – ■■

Conversion of Cellulose and Cellobiose into Sorbitol Catalyzed by Ruthenium Supported on a Polyoxometalate/Metal–Organic Framework Hybrid

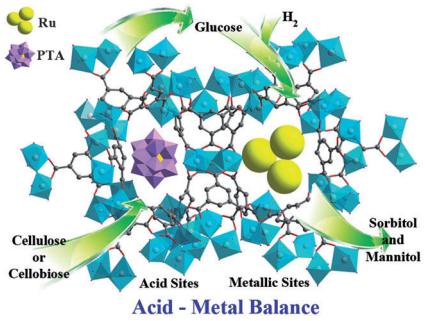

Acid/Metal Balance: Bifunctional catalysts containing ruthenium and polyoxometalates as active species with a metal-organic framework as support and encapsulation matrix, respectively, are synthesized. Excellent yields in sorbitol are obtained in the conversion of cellobiose and ball-milled cellulose. The evaluation of the balance between the hydrogenation and hydrolysis functions of these bifucntional catalysts reveals that by carefully balancing the ratio of acid site density and the number of metal surface atoms a maximum conversion can be achieved.